ANALYSIS OF THORACIC IMPACT RESPONSES AND INJURY PREDICTION BY USING FE THORACIC MODEL

Lenka Číhalová*

The previously developed thoracic finite element model [8, 9] was used to investigate the human thoracic dynamic responses associated with the frontal, lateral and oblique loading and to predict injuries of the thorax associated with the frontal loading. The thoracic model was developed [8, 9] to improve the human articulated rigid body model ROBBY (the model of an average adult male) [13, 14], which was previously developed at the University of West Bohemia in cooperation with ESI Group (Engineering Simulation for Industry). There are implemented deformable models of the thorax and abdomen in the ROBBY model. The geometries of individual thoracic organs were based on the cadaver tomography data and color cross-section photographs obtained from Visible Human Project (VHP) [33]. The thoracic model material properties were obtained either by virtue of cooperation with ESI Group or from public sources (articles, Internet, books). Thoracic model includes the models of the sternum, ribs, costal cartilages, vertebrae, lungs, heart, trachea, main vessels (aorta, vena cava superior), intercostal muscles, diaphragm, flesh and skin. The presented study deals with the dynamic response and validation of the whole thoracic model and with the prediction of thoracic injuries by virtue of this model. The results of simulations are compared with the experimental results.

Keywords: *biomechanics, thoracic model, validation, frontal, lateral and oblique impactor test, injury criterion*

1. Introduction

The thorax is one of the most vulnerable part of the human body. For a long time the impact injury of the thorax has been the subject of extensive research [4, 18, 22, 17, 32], etc. Many studies have been focused on the identification of effective injury criteria [7, 30, 31], etc.

For the evaluation of the thoracic response and injury arising during the impact, it is very important to determinate the surrogate, which is able to represent the human body [16]. The analytical and computer models, human volunteers, animals and cadaver have been previously utilized to represent surrogates of vehicle occupants to investigate the thoracic response by many experts. Each of these surrogates has some advantages and disadvantages. Human volunteers have the accurate anatomy and physiology, but may not be used for injuries testing. Animals can be used for injuries testing, however they are anatomically different from a human body. Computer models are limited in the available data necessary for the validation. Therefore for injuries testing, a human cadaver (also called post mortem human subjects (PMHS)) are assumed as the closest surrogates of the living human due to its anatomical similarity and similar hard-tissue injury potential [16]. These are also

* Ing. L. Číhalová, Ph.D., New Technologies Research Center, University of West Bohemia, Univerzitní 8, 306 14 Plzeň, Czech Republic

fundamental for the validation of computer models, which can be used for the prediction of injuries. Computer models also offer the possibility for more detailed observations of the stress and strain of the human organs compared to those that are possible to obtain with cadavers and dummies, where only the information from the chest deflection and spine acceleration can be used to predict the thoracic injury [5].

2. Thoracic model description

Author previously developed the thoracic model [8, 9], which is based on the real anatomical human data, since CT photographs and color photographs from VHP [33] were used. For detail description of geometry creation and model completion see [8]. The geometry was completed by the material properties either obtained due to the cooperation with ESI Group or from several public sources [10, 26, 34], etc. Hence two types of thoracic models were created. The individual organs in the thoracic model were covered by thin layers. These thin layers have the purpose of contact interfaces between the particular organs. There were used two types of contacts: i) sliding contact, which models the mutual contact of organs, ii) tied contact representing the ligaments. The correct movement of the spine is ensured by the definition of joints: i) among individual vertebrae and ii) between rib and corresponding vertebra.

2.1. Individual thoracic organ models

In the biological reality the hollow organs are usually filled by some fluid. This fact was simplified in the thoracic model. Therefore the organ of lung exhibiting the elastic behavior and the organ of heart exhibiting the viscoelastic behavior in the relax state were simulated by the set of standard three dimensional solid elements [24]. Consequently, to save the computational time, the organs were modeled as biobags [12] with the fluid inside, i.e. with water in the case of heart and with air in the case of lung. Both types of variants (solid and biobag) were applied in the thoracic model to simulate the organ of lungs and heart. Firstly, the standard three dimensional solid elements were used to simulate all thoracic organs, only the abdomen was created as biobag with the water inside to fill the abdominal cavity and to ensure the connectivity of the whole generated model. This model is in the whole study called the *'solid model'*. Consequently, the second type of model the *'biobag model'* was created. There are all organs simulated in the same way as in the case of solid model, only both lungs and the heart were simulated as biobags. These models are completed with public material data. By the same way the 'ESI solid model' and 'ESI biobag model' were created. There were used the material properties obtained in cooperation with ESI Group. Because of copyright it was necessary, for the following publication of the thoracic model, to include the material properties obtained not only in the cooperation with ESI Group, but also from the public sources. The constitutive laws for all organs are either considered as elastic, elastic-plastic or viscoelastic [9].

The volumes of the individual organs were constructed by virtue of the set of mainly hexahedral solid elements [24]. There are only a few tetra solid elements, pyramid solid elements and penta solid elements [24]. They were used in the places with not simple geometry, where it was not possible to use hexahedral elements. Number of nodes in thoracic model is 22807 and number of solid elements in thoracic model is 11187. The surfaces of the individual organs were created by using mainly quad shell elements [24]. There were utilized only a few tria shell elements [24]. The detailed description of thoracic model can be found in [9].

The geometry of thoracic model was created in the Amira software [3], which is an advanced software system for 3D visualization, data analysis and geometry reconstruction. It is widely used in many areas such as microscopy, medicine, biology, or engineering. Its great advantage is the ability to create the 3D object model from the cross-section through the surveyed object. The models of individual thoracic organs obtained from Amira software were remeshed and modified in HyperMesh software [2]. Whole model of thorax was completed (definition of material properties, contacts and joints) in PAM-CRASH$^{\mathrm{TM}}$ software [24], where it was also validated.

3. Thoracic model validation

The created thoracic model was validated against the frontal (Kroell et al. [18, 19, 20]), the lateral (Boquet et al. [4]) and the oblique (Viano et al. [31, 32]) loading. All of these tests are based on the experimental tests, which investigated the response of human body during different impact conditions. The validation process was done through the comparison of the resultant impactor force-chest deflection dependencies of simulations and cadaver tests.

Experimental tests were previously performed by specialists during various impact conditions with various human bodies [4, 18, 19, 20, 31, 32]. Therefore the results of these experiments had to be normalized and statistically processed to establish the response of average man. This response is described by virtue of corridors of dependency total impactor force-chest deflection during various impact conditions. Corridors are composed by lower curves and upper curves, which enclose them. The aim of the validation of virtual biomechanical model, i.e. the checking of the reality of the model, is to have the similar response of the virtual model as response of human body, i.e. the belonging of simulation results into the corridors.

3.1. Validation of thoracic model by the frontal pendulum test

The validation in the frontal direction was performed on the basis of the experimental tests, which were performed by Kroell et al. in 1970's [18, 19 20, 22] with cadavers. The following setup describes the performance of frontal validation tests.

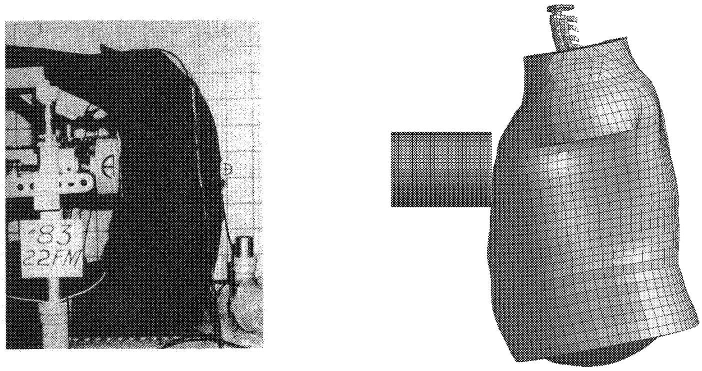

Fig.1: The setup of the frontal pendulum thoracic test: the experiment [20] and simulation

The setup of the frontal test according to [21, 23], see Figure 1:

1. A rigid and flat impactor with a 150 mm in diameter and mass of 23.4 kg is used.
2. The subject is set up in sitting position, with no back support.
3. The subject is positioned in front of the impactor.
4. The center line of the impactor aims to mid-line of the sternum between 4th and 5th rib.
5. The impact speed during the test is 4.9 m/s, 6.7 m/s, and 9.9 m/s, respectively.

The both, experiment and simulation configuration are visualized in Figure 1. The simplification of the surveyed model (see Figure 1) in comparison with the experiment, where the tests were performed with the whole human cadaver body, was performed. However it must be mentioned that this restriction of model imperceptibly influences the results of thoracic model validation, see [15]. Hence the left, right leg, the abdomen and the pelvis were replaced by the additional mass called the 'bottom' corresponding with the mass of the legs, the pelvis and the abdomen. The left and right hand and the head were replaced by additional masses corresponding to mass of hands and head. The aim of this addition of the mass was to preserve the mass of the whole human body. The values of these additional masses according to [24] are described in Table 1.

Name of added mass	**Added mass** [kg]
Head	4.8
Left hand	3.5
Right hand	3.5
Bottom (abdomen, pelvis, legs)	27.0

Tab.1: The values of added masses

The left hand side of Figure 1 illustrates the way to apply blunt sternal loading to the cadaver specimens. The subject was seated in front of the impactor with arms outstretched and lightly taped to horizontal position to keep the torso posture in the correct position. During the impact, this minimal restraint was broken with the negligible effect upon the resulting whole body kinematics [21].

During the validation the time dependency of frontal chest deflection and impactor force were investigated and they were utilized to compare the results of the simulation and experiment. Generally, the posterior displacement of the anterior chest under the frontal loading is often used to describe the thoracic injury risk [17]. This displacement is commonly called as the *chest deflection*. Results of the validation, i.e. the impactor force-chest deflection dependencies for two types of material properties definitions (obtained either in the cooperation with ESI Group, or from public sources) with both variants of organs definition (solid and biobag), are visualized in Figures 2 and 3.

The force-deflection dependencies, which are hysteresis curves, are visualized in Figures 2 and 3. Such curves can be divided into the loading and unloading phase. The loading phase is characterized by an initial rapid rise, which is mainly caused by viscous properties of the thorax. As can be seen in Figures 2 and 3 this phase shifts to higher values of the deflection with the increasing impact speed, i.e. during 4.9 m/s impact speed the force increases to approximately 20–30 mm of deflection, however during 9.9 m/s the force is increasing to 40–50 mm of the deflection. The plateau region is also the result of the viscous response. This phase is also influenced by the impact speed, since during 4.9 m/s impact speed it runs to 70–80 mm of the deflection, in case of 9.9 m/s impact speed this phase finishes in

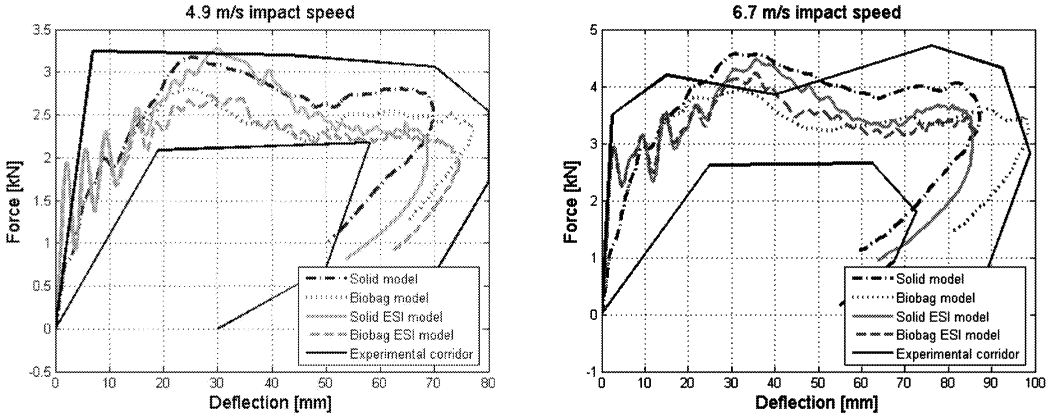

Fig.2: Results of the frontal validation for impact speed 4.9 m/s and 6.7 m/s

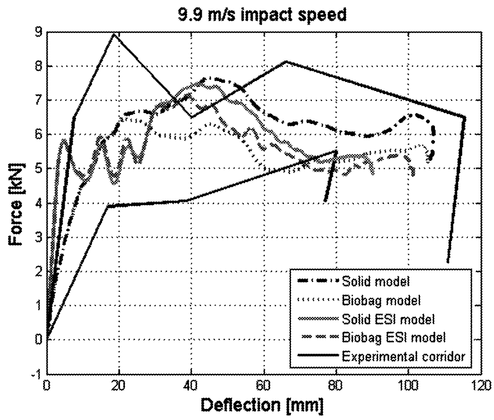

Fig.3: Results of the frontal validation for impact speed 9.9 m/s

the neighborhood of 100 mm of chest deflection. Finally, the unloading phase represents the unloading of the compressed tissues and follows the elastic non-linear unloading of the thorax [27].

The results of dependencies of the impactor force-chest deflection (see Figures 2 and 3) are similar in loading phase for all four types of models. There are only small differences in the phase of plateau and the unloading phase. However, they are still in the agreement with experimental results.

3.2. Validation of thoracic model by the lateral pendulum test

Recently, to investigate the biomechanical response of the human body in the lateral impact [4], the same methods used to analyze the frontal loading have been applied. The cadaver studies have been performed to investigate the behavior during such loading. As a result of these impactor tests, hysteresis curves have been presented. They have been similar to those obtained for the frontal loading except for the fact that no or less apparent force plateau regions have been determined [27]. Furthermore, it has been shown that the resistance of the thorax to the lateral impact is smaller than to the frontal loading [27].

However, it must be said that the arm can have the protective effect when it is positioned between the striking object and the thorax [27].

A few lateral tests with cadavers were conducted by Bouquet et al. [4], to investigate the behavior of the thorax during the loading in the lateral direction. INRETS [12] performed a few similar tests according to same setup described bellow. The force-deflection dependencies were determined as the results of these experiments. The data were processed and corridors of force-deflection dependencies for impact speed 3.3 m/s and 5.9 m/s were created [12], see Figure 5. These were also utilized during the validation of thoracic model in the lateral direction to compare the results of simulations and experiments, see Figure 5.

The setup of the lateral test according to [4, 28], see Figure 4:

1. The subject is set up in the sitting position.
2. The impactor axis is horizontal, centered to the center of thorax gravity at the level of T8/T9 under armpit.
3. The impact speed during tests is 3.3 m/s and 5.9 m/s, respectively.

This setup was used to prepare the simulation for the validation in the lateral direction. Both, the scheme of the experiment and simulation are visualized bellow, see Figure 4.

The impactor force-lateral chest deflection dependencies, which are hysteresis curves are visualized in Figure 5. The phase of plateau is negligible during the simulation with 3.3 m/s

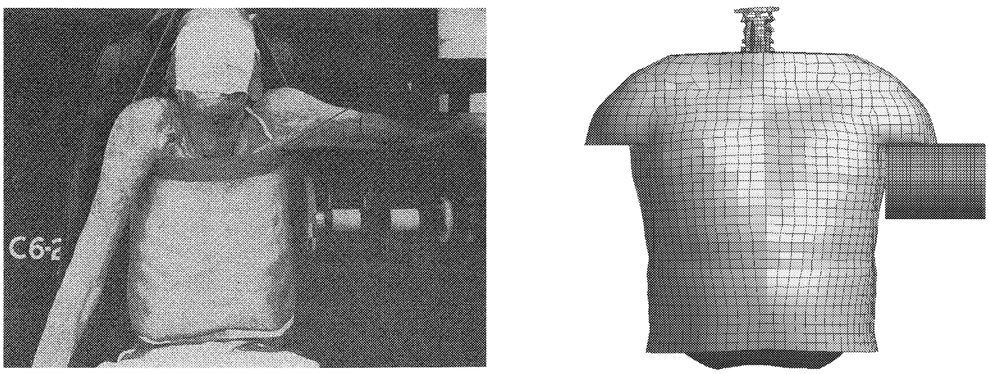

Fig.4: The setup of the lateral test: experiment [28] and simulation

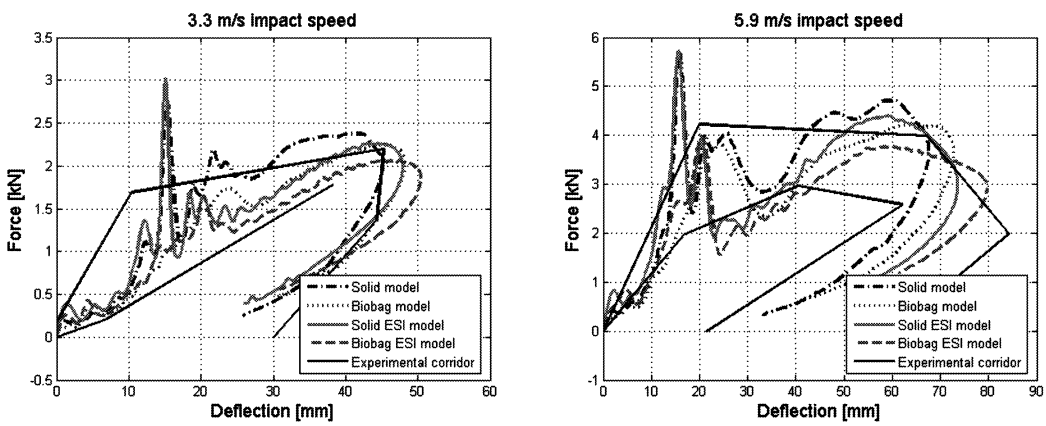

Fig.5: Results of the lateral validation for impact speed 3.3 m/s and 5.9 m/s.

impact speed. The results of all four models are similar in the phase of loading, however in the phase of unloading there are some dissimilarities. Between 10 and 20 mm of lateral chest deflection the sudden increase of impactor force can be observed for both types of tests. This is caused by the response of the soft organs, such as lungs and the heart, which are created in both variants (solid and biobag). As can be seen, in biobag variants there is no such peak visible. It is caused by the fact that the 'solid model' has greater stiffness than 'biobag model'. However, the results in the plateau and unloading phase are in very good agreement with experiments.

Moreover, the thoracic model is more resistant in the frontal impact than in the lateral impact, see Figure 2 and 5.

3.3. Validation of thoracic model by the oblique pendulum test

Thoracic cadaver oblique impacts conducted by Viano et al. [31, 32] were simulated to validate the thoracic model in the oblique direction. On the base of his study there were previously determined the corridors of force-deflection dependencies [31]. The tests were performed according to following setup.

The setup of the oblique test according to [31, 32], see Figure 6 :

1. The subject is in a standing position.
2. The impactor has a horizontal axis, centered on the thorax with a 30° angle.
3. The impact is delivered at the level of the xiphoid process, 7.5 cm under the sternum center.
4. Impactor is rigid with 150 mm in diameter and mass 23.4 kg.
5. The impact speed during the tests is 4.42 m/s, and 6.52 m/s, respectively.

Both, the experiment and simulation configuration are visualized bellow, see Figure 6.

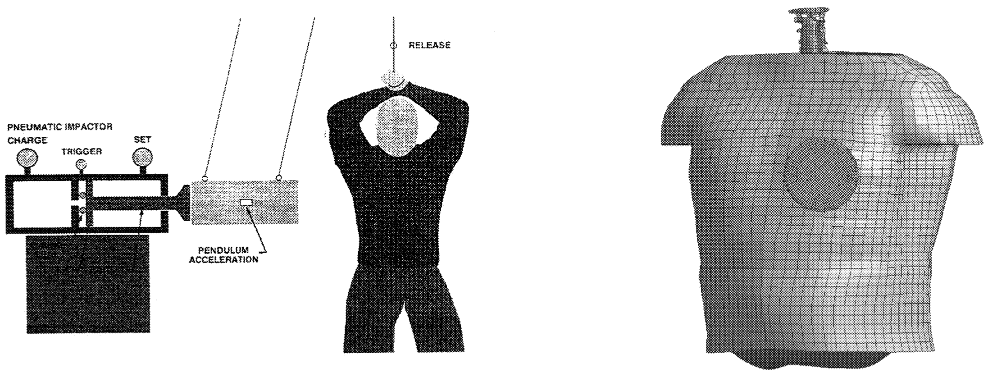

Fig.6: Experimental set-up of the oblique test with pneumatic power-assisted pendulum and upright supported specimen [31] and the setup of the oblique simulation

The force-deflection dependencies for both impact speeds as the results of simulations, were compared with corridors representing the results of experiments, see Figure 7.

The force-deflection dependencies are again hysteresis curves, see Figure 7. However in the comparison with lateral test the plateau phase is here apparent. The resistance of the thorax in the frontal impact is again more resistant than during the oblique impact. In the

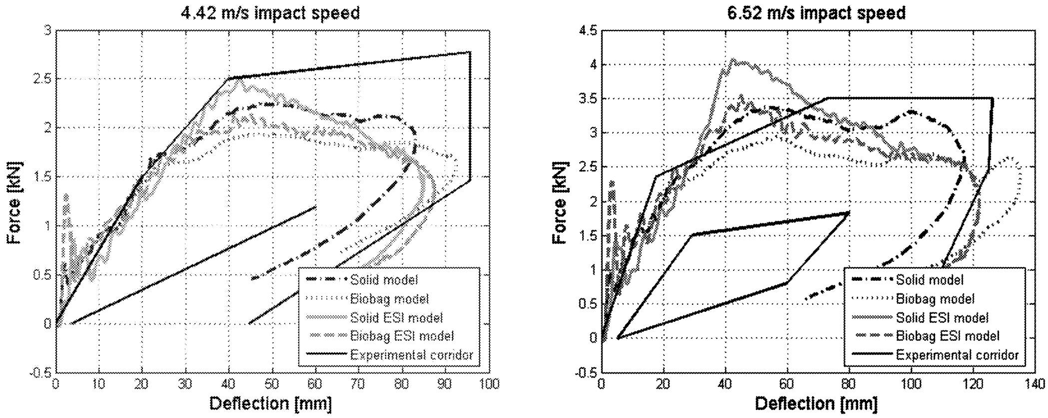

Fig.7: Results of the oblique validation for impact speed 4.42 m/s and 6.52 m/s

loading phase, the results are similar for all four types of models. In the phase of plateau and unloading the responses are little different. However, they are still in agreement with experimental results.

4. Injury prediction

Injury prediction during the frontal pendulum loading was performed on the base of elementary thoracic injury criteria (important measures to assess the severity of impacts and the risk of sustaining injury). An injury criterion correlates a function of physical parameters (e.g. acceleration, force) with a probability of certain body regions to be injured. Injury criteria are generally proposed and validated on the basis of experimental studies [27].

Several tests with various impact conditions in the frontal direction (see Table 2) were performed with the impactor of 150 mm in diameter to analyze the response of the developed validated thoracic model. 'Solid model' with public material properties was taken into account. The center line of the impactor aimed to mid-line of the sternum between 4th and 5th rib. These simulation tests were based on the study [26], which compared the responses of their human body model with the responses of cadaver tests performed by Kroell [19].

Test name	Impactor mass [kg]	Impactor speed [m/s]	Impact energy [J]
F14	22.91	7.33	615.5
F22	23.64	6.70	530.6
F25	5.50	13.80	523.7
F26	1.86	11.20	116.7
F28	1.64	14.50	172.4

Tab.2: Experimental input values – the number after 'F' denotes the test number in the Kroell study [22]

Firstly, the chest deflection was investigated. It was measured between two points in the transverse plane, with one point in the impact side (anterior part of the thorax) and the other point in the side opposite to the impact (posterior part of the thorax). Consequently, the rate of deflection V was calculated from the chest deflection by the time derivative. The compression of chest C was computed by the division of deflection $D(t)$ by initial depth of the thorax b. Finally, the chest deflection and its rate were used to determine VC according to the equation (1).

$$VC = V(t)\,C(t) = \frac{\mathrm{d}[D(t)]}{\mathrm{d}t}\,\frac{D(t)}{b}\ . \tag{1}$$

The viscous criterion VC (velocity of compression) [27], also called *the soft tissues criterion*, is an injury criterion for the chest area taking into account that the soft tissue injury is compression-dependent and rate-dependent. On the other hand the maximal compression of the chest is the determining factor for rib fractures. Moreover the number of rib fractures depends on the magnitude of rib deflection, rather than the rate of deflection [6].

The maximal value of the velocity of compression VC_{max} is simply the maximum value of VC over the impact time interval.

$$VC_{\mathrm{max}} = [V(t)\,C(t)]_{\mathrm{max}}\ . \tag{2}$$

Table 3 lists the maximal computed values of the compression C_{max}, the velocity V_{max} and the viscous response VC_{max} of thoracic model for all the impact conditions given in Table 2. Moreover according to [6], who found that the compression $> 20\,\%$ regularly produced rib fractures [6], the probability of rib fractures was estimated.

Test name	C_{max} [%]	V_{max} [m/s]	VC_{max} [m/s]	**Probability of rib fractures according to C_{max}**
F14	44	7.3	1.41	high
F22	41	6.7	1.27	high
F25	36	13.8	1.60	high
F26	9	11.2	0.32	minimal
F28	16	14.5	0.67	low

Tab.3: The maximal value of compression, velocity and viscous response of simulated tests

In general, the value of V_{max} increased with impact speed, while the value VC_{max} increased with the impact energy, see Table 3.

Consequently, the values of AIS (Abbreviated Injury Scale) [1] according to the equation (3) were determined, see Table 5.

$$\mathrm{AIS} = -3.78 + 19.56\,C_{\mathrm{max}}\ . \tag{3}$$

AIS is the standard method for classifying the level of injury of a body region or organ. It was created on the base of the demand for widely accepted injury scale that could be used by the medical engineering automotive accidents investigation teams to classify the level of injury [29]. Today it is used for the prediction of research and assessments during emergency medical situations.

The AIS uses a numerical rating system to assess the impact injury severity. The scale starts with 0, in case when any injury can occur and finishes by six, when the possibility of the survival is negligible. Therefore the greater AIS number indicates the greater severity of the injury. The scale does not quantify the long-term disability or medical and societal costs of the injury. Deviation of Abbreviated Injury Scale is described in Table 4.

AIS Level	Injury severity
0	No injury
1	Minor
2	Moderate
3	Serious (not life threating)
4	Severe (life threating but survivable)
5	Critical (survival uncertain)
6	Fatal

Tab.4: AIS ranking codes according to [27]

Test name	AIS from compression	Probability of AIS [%]
F14	5	P(AIS 5) = 1
F22	4	P(AIS 4) = 28
F25	3	P(AIS 3) = 46
F26	0	
F28	0	

Tab.5: AIS according to the maximal compression and the probability of AIS

Test name	Number of rib fractures	AIS from rib fractures
F14	9	4
F22	8	4
F25	4	3
F26	0	0
F28	0	0

Tab.6: AIS according to the number of rib fractures

AIS Skeletal Injury	AIS Soft tissue injury
1 one RF	**1** contusion of bronchus
2 2–3 RF; sternum fracture	**2** partial thickness bronchus tear
3 4 or more RF on one side; 2–3 RF with HT or PT	**3** lung contusion minor heart contusion
4 fail chest; 4 or more RF on each two side, 4 or more RF with HT or PT	**4** bilateral lung laceration; minor aortic laceration; major heart contusion
5 bilateral flail chest	**5** major aortic laceration; lung laceration with tension PT
	6 aortic laceration with hemorrhage not confined to mediastinum

RF – rib fracture,
HT – hemothorax (bleeding into the pleural space)
PT – pneumothorax (if a hole is created in the pleural sac between the lungs and the rib cage)

Tab.7: AIS rating for the skeletal and soft tissue injury [1]

Not only maximal value of compression C_{max}, but also the number of rib fractures is the indicator of AIS. The amount of rib fractures during the individual impact condition is summarized in the Table 6 bellow. The corresponding AIS according to the Table 7 is also presented.

Table 7 represents the typical AIS of injuries of the rib cage and thoracic soft tissues.

The number of rib fractures in the thoracic model could be investigated due to fracture model capability. There was used the failure stress of ribs equals to 85 MPa according to [34].

As can be seen from the Tables 5 and 6 the values of AIS determined from the C_{max} and from the number of rib fractures are almost identical. The difference was observed only in case of the test F14.

The placement of the rib fractures during tests F14, F22 and F25 together with von Misses stress analysis, which is represented in the time of maximal compression, is visualized in Figures 8, 9 and 10.

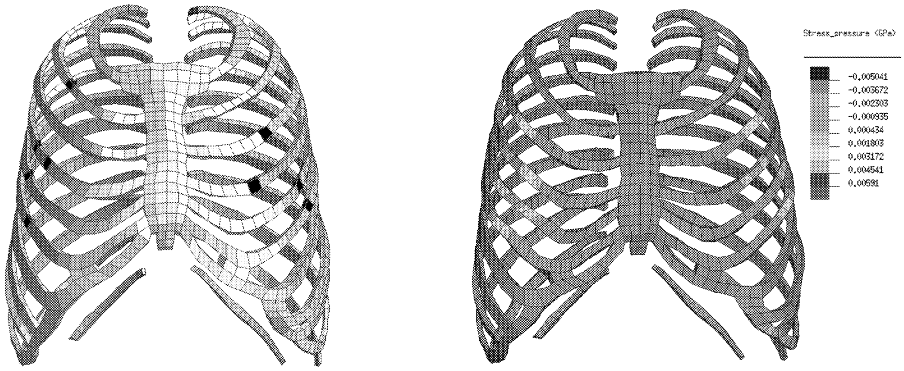

Fig.8: Rib fractures of the test F14 and the stress distribution in [GPa] in 24 ms

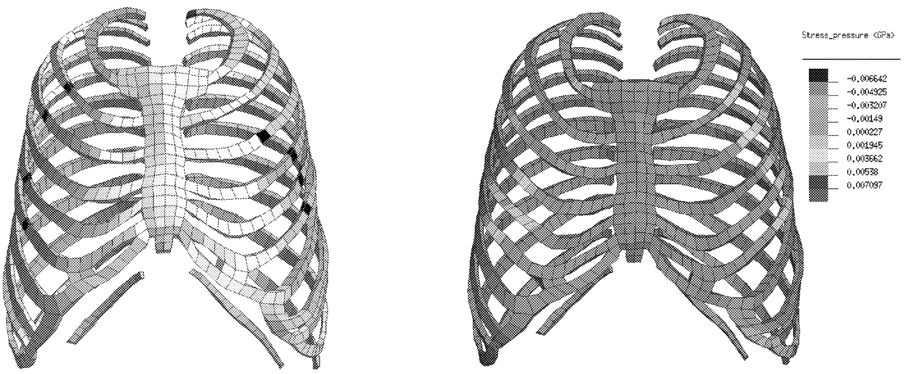

Fig.9: Rib fractures of the test F22 and the stress distribution in [GPa] in 24 ms

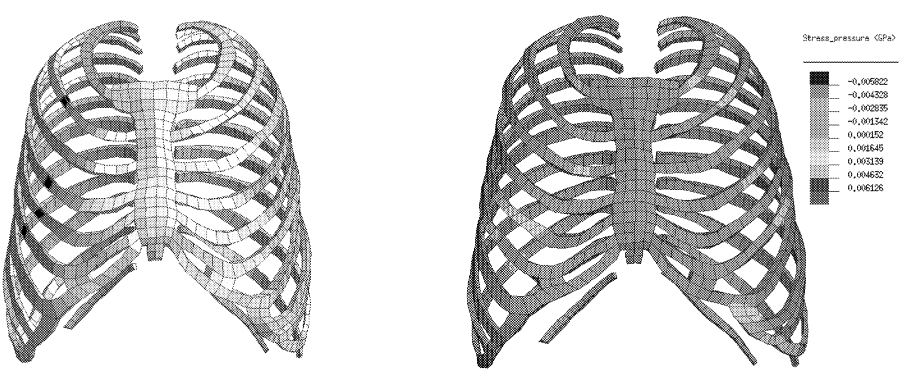

Fig.10: Rib fractures of the test F25 and the stress distribution in [GPa] in 12 ms

In these tests, the fractures occur predominantly in the second, third, fourth, fifth and six rib. Moreover, during the test F25 with lower impact energy, the fractures occur only on the right side. This is in agreement with cadaver tests, where the more frequent fractures were the fractures of the second right and third right rib [26].

By comparing both types of figures, i.e. the figure with rib fractures and the stress distribution, it is apparent that the fractures occur in the places of stress concentrations.

In conclusion, the comparison of the responses of cadaver tests according to Kroell [19] and the 'solid model' of thorax is presented in Table 8.

Test name	**Cadaver tests**			**Simulation**		
	$C_{\max}$ [%]	$V_{\max}$ [m/s]	$VC_{\max}$ [m/s]	$C_{\max}$ [%]	$V_{\max}$ [m/s]	$VC_{\max}$ [m/s]
F14	42	6.5	1.72	44	7.3	1.41
F22	42	6.0	1.58	41	6.7	1.27
F25	39	13.0	2.27	36	13.8	1.6
F26	18	10.5	0.68	9	11.2	0.32
F28	23	12.0	1.08	16	14.5	0.67

Tab.8: The comparison of cadaver test injuries and simulation test injuries

From this table it can be concluded that the results are similar, but not equal. The evaluation of the thorax response strongly depends on the tested subject. Due to variability of specimens in age, sex, material properties, weight, height, and other dimensions, the cadaver impact responses vary from test subject to test subject, even in the same impact conditions [26].

Since cadavers in experiment were in various age range (old, young), the comparison of injuries of cadaver and model, where the material properties represent average behavior of tissue, is not comparable. Therefore there are great differences of model and cadaver results in case of the rib fractures, see Table 9.

	Cadaver tests		**Simulation**
Test name	**Age** [years]	**Number of rib fractures**	**Number of rib fractures**
F14	67	22	9
	81	22	
	76	7	
F22	78	12	8
	19	0	
	29	0	
F25	65	18	4
F26	75	0	0
F28	54	0	0

Tab.9: The comparison of number of rib fractures for cadaver test injuries according to Kroell [19] and simulation test injuries

As can be seen from the Table 9 the number of fractured ribs is different during the same impact conditions. Hence the values of failure stress are not uniform for all individuals. It is connected with experimental investigation, when Granik and Stein [11] reported that the failure stress for a normal rib ranges from 75 to 137 MPa. However for abnormal ribs the failures stress can be as low as 6 MPa.

5. Conclusion

Validation of thoracic model

The aim of this study was to investigate the response of previously generated thoracic model [8, 9] during various impact conditions. Validation of four types of thoracic model, i.e. 'solid model', 'biobag model', 'ESI solid model', 'ESI biobag model', was performed by the frontal, lateral and oblique pendulum tests, which were based on the experimental tests performed with cadavers [4, 18, 19, 20, 31, 32]. The process of the validation was performed in the *PAM-CRASH*™ *software* [24]. The computed resultant impactor force-chest deflection dependencies were compared with the experimental results to validate the generated thoracic model. The results of the validation in three directions of the impact are in very good agreement with the experiments. Therefore the thoracic model can be used to investigate the response of the thorax in the crash simulation, where the impact is initiated from various directions. The advantage of biobag models is that they save the computational time. Disadvantage of the thoracic model is that it describes the behavior of an average man, with average proportions of body and simplified description of a complex organ behavior. Therefore for the investigation of response of concrete individual the some adjustments, such as scaling and detailed searching of the organ material description, would be necessary. Following improvement of the thoracic model can be also the integrating of muscle tense, which increases the body rigidity.

The thoracic model has also the possibility to predict injuries of thorax. These can be predicted from the acceleration of spine, force applied to the torso, etc. Moreover, since the thorax is modeled as deformable, the thorax injury can be predicted from the chest deflection and injuries of thoracic organs can be predicted by using stress-strain analysis. Thoracic model has also the possibility to predict the rib fractures.

Injury predictions

To analyze the elementary indices of injury, such as the compression C, velocity of deformation V and viscous response VC of thorax, five frontal pendulum tests with various impact conditions were performed. Initial conditions of these tests were based on the study [19]. The maximal values of C, V and VC obtained during the simulation were compared with the experimental ones according to [19]. The values of the simulation and experiments were similar. However there were some differences caused by the individuality of particular tested subject. This was caused by the differences in age, sex, proportions, etc. of individuals. Consequently, on the basis of the maximal values of $C_{\max}$ in the individual tests the values of Abbreviated Injury Scale (AIS) were determined. Moreover, since the model of ribs is able to predict the rib fractures, the value of AIS from the number of rib fractures was established. The number of computed rib fractures was compared with the experiments. However, this item is not exactly comparable, since the number of rib fractures strictly dependents on the material properties of ribs. And these differ from specimen to specimen very much. Whereas von Misses of 40 MPa would indicate rib fractures for older cadavers (age 65–81), under the same condition rib fractures do not occur for young people [26].

Acknowledgment

This study was supported by John H. and Anny Bowles Foundation and by ESI Group International.

References

[1] Abbreviated Injury Scale (AIS) – 1990 Revision, American Association for Automotive Medicine, Morton Grove, IL, 1990

[2] Altair® HyperMesh®7.0, Online: http://www.altair.com/software/hw hm.htm

[3] Amira, Version 3.1, User's guide, 2002

[4] Bouquet R., Ramet M., Bermond F., Cesari D.: Thoracic and human pelvis response to impact, proceedings of the 14th International technical conference on enhanced safety of vehicles, pp. 100–109, 1994

[5] Campbell J.Q., Tannous R.E., Takhounts E.G., Martin P., Eppinger R., Nguyen: On the development of a theoretically based, statistically justified, thoracic injury criterion

[6] Cavanaugh J.M.: Accidental injury: biomechanics and prevention, Biomechanics of Thoracic Trauma, Chapter 16, New York: Springer, 2002

[7] Cavanaugh J.M., Zhu Y., Huang Y., King A.I.: Injury and response of the thorax in side impact cadaveric tests, Proc. 37th Stapp Car Crash Conf., pp. 199–221, 1993

[8] Číhalová L.: Development of biomechanical deformable thoracic model, Journal Engineering mechanics, Vol. 13, No. 6, pp. 453–465, 2006

[9] Číhalová L.: Biomechanical models of tissue and their implementation into human body, PhD thesis, Plzeň, (2008)

[10] Furusu K., Watanabe I., Kato Ch., Miki K., Hasegawa J.: Fundamental study of side impact analysis using the finite element model of the human thorax, Bio mechanics laboratory, Vehicle Engineering, Japan, Vol. 22, pp. 195–199, 2001

[11] Granik G., Stein I.: Human ribs: static testing as a promising medical application, Journal of Biomechanics, Vol. 6, pp. 237–240, 1973

[12] Haug E., Choi H.Y., Robin S., Beaugonin M.: Human models for Crash and Impact Simulation, Special Volume of Handbook of numerical analysis, vol. XII, Editor – P.G.Ciarlet, pp. 231–670, 2004

[13] Hynčík L.: Human articulated rigid body model (ROBBY1), ESI SA, (1997)

[14] Hynčík L.: Biomechanical Human Model, Biomechanics of Man, (2000)

[15] Hynčík L.: Biomechanical model of abdominal organs and tissue for car crash test purposes, PhD Thesis, University of West Bohemia, Pilsen, 2002

[16] Kent R.: Dynamic Response of the Thorax: Restraint-Specific Injury Prediction and Constitutive Description, PhD thesis, University of Virginia, 2001

[17] Kent R., Patrie J., Poteau F., Matsuoka F., Mullen Ch.: Development of an age-dependent thoracic injury

[18] Kroell C.: Thoracic response to blunt frontal loading, 'Biomechanics of impact injury and injury tolerances of the thorax-shoulder complex', edited by Backaitis S.H., published by Society of Automotive Engineers, Inc., pp. 51–80

[19] Kroell C.K., Schneider D.C., Nahum A.M.: Impact tolerance and response of the human thorax, SAE 710851 15th Stapp car crash conference, 1971

[20] Kroell C.K., Schneider D.C., Nahum A.M.: Impact tolerance and response of the human thorax II, SAE 741187 18th Stapp car crash conference, 1974

[21] Lobdell T.E., Kroell C.K., Schneider D.C., Hering W.E., Nahum A.M.: Impact response of the human thorax, pp. 201–245, Plenum Press, New York, NY, 1973

[22] Nahum M., Schneider D.C., Kroell C.K.: Cadaver skeletal response to blunt thoracic impact, SAE Paper751150, Proceeding of the 19th Stapp Car Crash Conference, 1975

[23] Neathery R.F.: Analysis of chest impact response data and scaled performance recommendations, SAE paper 741188, Proceedings of the 18th Stapp Car Crash Conference, Ann Arbor, MI, 1974

[24] PAM-CRASH/SAFE™, Notes Manual, Version 2004

[25] Robbins, D.H.: Anthropometry of Motor Vehicle Occupants, Vols. 2–3, University of Michigan, UMTRI-73-73-2, 1973

[26] Ruan J., El-Jawahri R., Chai L., Barbat S., Prasad P.: Prediction and Analysis of Human Thoracic Impact Responses and Injuries in Cadaver Impact Using a Full Human Body Finite Element Model, Stapp Car Crash Journal, Vol. 47, pp. 299–321, 2003

[27] Schmitt K.-U., Niederer P., Walz F.: Trauma biomechanics, Introduction to accidental injury, Springer-Verlag Berlin Heidelberg New York, 2004
[28] Stalnaker R.L., Roberts V.L., McElhaney J.H.: Side impact tolerance to blunt trauma, Proceedings, 17th Stapp Car Crash Conference, pp. 377–408, 1973
[29] States J.D. : The abbreviated and the comprehensive research injry scales, Proceedings of 13th Stapp car crash conference, 690810
[30] Tarriere C., Walfish G., Fayon A.: Synthesis of human tolerances obtained from lateral impact simulations, Proc. 7th Intern. Techn. Conf. on Experimental Safety Vehicles, pp. 359–373, 1979
[31] Viano C.V.: Biomechanical responses and injuries in blunt lateral impact, SAE Paper N°902310, Proceedings of the 33th Stapp Car Crash Conference, pp. 113–42, 1989
[32] Viano D.C., Lau I.V., Asbury C.: Biomechanics of the human chest, abdomen, and pelvis in lateral impact, Accident; analysis and prevention, Vol. 21, pp. 553–74, 1989
[33] Visible Human Project®, U. S. National library of medicine, 2003
Online: http://www.nlm.nih.gov/research/visible/visible_human.html
[34] Zhao J., Narwani G.: Development of a human body finite element model for restraint system R&D applications, TAKATA – Automotive System Laboratory, Inc., paper number 05-0399

Received in editor's office: June 13, 2008
Approved for publishing: October 14, 2008